JOURNAL OF THE AMERICAN WATER RESOURCES ASSOCIATION
VOL. 35, NO. 5 AMERICAN WATER RESOURCES ASSOCIATION OCTOBER 1999

DEFINING WATERSHED-SCALE EVAPORATION USING A NORMALIZED DIFFERENCE VEGETATION INDEX[1]

Jozsef Szilagyi and Marc B. Parlange[2]

ABSTRACT: Monthly composites of the Normalized Difference Vegetation Indices (NDVI), derived from the National Oceanic and Atmospheric Administration's (NOAA) Advanced Very High Resolution Radiometer (AVHRR), were transformed linearly into monthly evaporation rates and compared with detailed hydrologic-model simulation results for five watersheds across the United States. Model-simulated monthly evaporation values showed high correlations (mean $R^2 = .77$) with NDVI-derived evaporation estimates. These latter estimates, used in a classical water balance model, resulted in equally accurate simulations of monthly runoff than when the model was run to estimate monthly evaporation via soil moisture accounting. Comparison of NDVI-derived evaporation estimates with pan data showed promise for transforming NDVI values into evaporation estimates under both wet and water-limiting conditions without resorting to the application of any kind of calibrated hydrologic models.
(KEY TERMS: watershed evaporation; vegetation index.)

INTRODUCTION

Evapotranspiration is the loss of water from the Earth's surface in vapor form. It occurs as evaporation from open water and moist soil surfaces and as transpiration from living plants. Since the physical process is the same in either case (i.e., vaporization of water), the term "evaporation" is usually adequate to cover all processes of vaporization (Brutsaert, 1982:1). In this paper the term "evaporation" is used unless specified otherwise. Evaporation is a fundamental part of the hydrologic cycle since on a global scale two-thirds of the precipitation over land surfaces is soon lost to it (Brutsaert, 1982:4). Reliable evaporation estimates are critical to the fields of hydrology, meteorology and climatology (Parlange *et al.*, 1995) because evaporation allows for the transfer of significant amounts of energy between the Earth's surface and its atmosphere. This efficient energy transfer is due to the large amount of latent heat involved in the vaporization of water, and as such, it has a great impact on the global circulation of the atmosphere and oceans and, consequently, on the Earth's climate (Luthi *et al.*, 1997). Global Circulation Models (GCM) describing the evolution of weather and climate turned out to be quite sensitive to the hydrologic budgets of the continents (Committee on Opportunities in the Hydrologic Sciences, 1991).

The various equations for estimating areal evaporation can be expressed in the following general form: $E = \alpha PE$, where E is actual and PE is potential evaporation (i.e., evaporation rate under unlimited water availability), and α is the Bodyko-Thornthwaite-Mather parameter (Parlange *et al.*, 1995). α is a function of soil moisture conditions and is unity until some measure of field capacity is reached, when its value decreases to zero with the drying of the soil (Parlange *et al.*, 1995). While evaporation estimates have been proven effective over relatively homogeneous terrain (in terms of vegetation, relief, soil type), at a scale smaller than 10^4 m (Crago and Brutsaert, 1992), their applicability at the watershed-scale (i.e., larger than 10^4 m) is hindered by uncertainties in estimating effective, watershed-representative values of the parameters involved in formulating E, since the parameter α itself is generally dependent on the spatial distribution of the soil-moisture content and the soil-plant-atmosphere relationships (Parlange *et al.*, 1995). One way to approach the problem of parameterization is the application of remotely sensed data.

[1]Paper No. 98152 of the *Journal of the American Water Resources Association.* **Discussions are open until June 1, 2000.**
[2]Respectively, Research Hydrologist and Assistant Professor, Conservation and Survey Division, University of Nebraska-Lincoln, Lincoln, Nebraska 68588-0517; and Professor of Hydrology, Department of Geography and Environmental Engineering, The Johns Hopkins University, Baltimore, Maryland 21218-2686 (E-Mail/Szilagyi: jszilagy@unlinfo.unl.edu).

In recent years, there has been much progress in estimating the parameters involved in evaporation calculations using remote sensing techniques. Studies estimating atmospheric parameters (i.e., near-surface air temperature, wind and water-vapor gradient) include applications of such remote sensing instruments as: (a) sodars (Quintarelli, 1993; Kaimal and Finnigan, 1994; Thomas and Vogt, 1993a,b); (b) radars (e.g., Ralph *et al.*, 1993); (c) and lidars (Galchen *et al.*, 1992; Eichinger *et al.*, 1993a,b, 1994; Parlange and Katul, 1995). While these techniques can be airborne or ground based, the remote sensing of general surface properties, such as surface temperature (e.g., Chen *et al.*, 1997; Smith *et al.*, 1997), surface soil moisture (e.g., Chen *et al.*, 1997; Chauhan, 1997; Jackson *et al.*, 1996), albedo (e.g., Lafleur *et al.*, 1997), and vegetative cover (e.g., Wittich and Hansing, 1995), all affecting evaporation, may also rely on satellite-based sensors, allowing for data acquisition at a much larger scale.

A detailed description of the regulatory role of vegetation in the process of transpiration has also been the focus of extensive multi-disciplinary research (e.g., Bunce, 1997; Desborough, 1997; Granier et al., 1996; Koster and Milly, 1997; Prazak *et al.*, 1996; Schreiber and Riederer, 1996). This is of special importance since transpiration makes up 90-95 percent of the total evaporation of vegetated surfaces (Maidment, 1993); thus defining transpiration rates provides a good estimate of evaporation over vegetated surfaces.

In the late 1970s, the application of remotely sensed vegetation indices for crop-yield monitoring and forecasting emerged (Tucker *et al.*, 1979). By the mid 1980s, an especially useful combination of the spectral response of vegetation in different wavelengths had been introduced and was given the name of "Normalized Difference Vegetation Index" (NDVI). NDVI is a combination of the spectral response of vegetation in the near-infrared (NIR; i.e. .73-1.1 μm for AVHRR data) and red bands (R; i.e., .55-.68 μm for AVHRR data) (Tarpley *et al.*, 1984)

$$NDVI = \frac{NIR - R}{NIR + R} \quad (1)$$

NDVI was demonstrated to be sensitive to changes in vegetation conditions since it is directly influenced by the chlorophyll's absorption of the sun's radiation (Tucker *et al.*, 1985). Because the chlorophyll status integrates the effects of numerous environmental factors, NDVI has been empirically related to the following components of the hydrological cycle over a wide range of spatial and temporal scales: soil moisture (Walsh, 1987; Henricksen and Durkin, 1986; Choudhury and Golus, 1988; Farrar *et al.*, 1994; Nicholson *et al.*, 1996), precipitation (Tucker *et al.*, 1985; Choudhury and Tucker, 1987; Seguin *et al.*, 1989; Nicholson *et al.*, 1990; Davenport and Nicholson, 1993; Schultz and Halpert, 1993; Di *et al.*, 1994; Nicholson and Farrar, 1994; Grist *et al.*, 1997; Yang *et al.*, 1997), and evaporation (Running and Nemani, 1988; Kerr *et al.*, 1989; Cihlar *et al.*, 1991; Gao *et al.*, 1992; Seevers and Ottmann, 1994; Nicholson *et al.*, 1996; Szilagyi *et al.*, 1998).

Running and Nemani (1988) regressed NOAA AVHRR-derived NDVI values against weekly forest evaporation rates calculated by an ecosystem model and found a linear relationship between the two. Kerr *et al.* (1989) applied NDVI values for the rainy season (June-September) of 1986 over Senegal to estimate evaporation, and found a strong linear relationship (R^2 = .98) between cumulative NDVI and the 20-day shifted evaporation, estimated by a water-balance model. Cihlar *et al.* (1991), applying a different water-balance model in Canada, found a similarly strong linear relationship (R^2 = .92) between the two variables, shifted by two weeks, using bi-weekly compilation periods for different soil type and vegetation combinations during the 1986 growing season (April-August). Gao *et al.* (1992) related six months of daily NDVI to the evaporative fraction (defined as the ratio of latent heat flux to the sum of latent and sensible heat fluxes) measured by fast response instruments at a single location during the First International Field Experiment (FIFE). Desjardins *et al.* (1992) related the greenness index (i.e., NIR/Red) of a 225 km^2 area to latent heat fluxes measured by an aircraft for selected days, also during FIFE. Seevers and Ottmann (1994) used thematic mapper NDVI values to estimate evaporation of different irrigated crops on selected days. Szilagyi *et al.* (1998) demonstrated that the NDVI versus evaporation relationship on a monthly basis is at least moderate (R^2 = .64) in a semi-arid environment as well, provided the hydrologic model-estimated evaporation data are shifted by one month later relative to the monthly mean NDVI values. Even the de-seasoned variables showed at least a weak correlation (R^2 = .28) suggesting that the NDVI-versus-evaporation relationship may not solely be a consequence of similar seasonal cycles of the two variables.

These studies demonstrated the applicability of NDVI for estimating evaporation at a single location, over a field or a watershed. As Wiegand and Richardson (1990) argued, a strong relationship between NDVI and evaporation should not, in fact, be surprising because the green plant tissue, of which chlorophyll activity is measured by NDVI (Sellers, 1985), must be active both photosynthetically and transpirationally. Note that the majority of the authors cited above do not differentiate between evaporation and transpiration in relation to NDVI. It should be pointed out, however, that NDVI can be physically related only to transpiration through Wiegand and Richardson's argument. The fact that NDVI relates to evaporation the same as it to transpiration is for reasons given earlier (i.e., transpiration is about 90 percent of the total evaporation of vegetated surfaces).

The above studies indicate a generally strong relationship between NDVI and evaporation, one that is linear or at least near-linear in nature. This means that NDVI values can be transformed into evaporation rates via a simple linear transformation. Below we show that NDVI-derived evaporation estimates result in simulated runoff of at least equal accuracy to classical water balance model estimates of both evaporation and runoff. This raises the question whether validating NDVI-derived evaporation values with hydrologic- or water balance-modeled estimates, as routinely done, is the best way to go, especially, when one can compare modeled runoff, obtained via the above-mentioned evaporation estimates (i.e. NDVI- and model-derived), with accurate observations.

HYDROLOGIC MODEL AND STUDY SITE DESCRIPTIONS

Two hydrologic models were used in this study. The first is a semi-distributed watershed model run on an hourly basis. For a detailed description of the model, see Szilagyi and Parlange (1999). The model divides the watershed into subcatchments according to stream-order and calculates simultaneous water balances on each subcatchment at an hourly increment. The model is computationally demanding and requires detailed descriptions of catchment geomorphology, stream network, soil types, land use/land cover types, and aquifer characteristics. Evaporation, (E) in the model is estimated by the following equation (Beven, 1991)

$$E = PE\left(1 - \frac{V_i}{V_{i0}}\right). \tag{2}$$

where V_i is the potential storage space of the soil. For a completely dry soil the maximum potential storage space V_{i0} can be estimated as

$$V_{i0} = fRDA \tag{3}$$

where f is the drainable porosity of the soil, RD is the rooting depth of the vegetation and A is the area of the specific soil type-vegetation combination. The potential evaporation (PE) is calculated as (Jensen and Haise, 1963)

$$PE = 0.016742 \cdot R \cdot (0.014 \cdot (1.8 \cdot T + 32) - 0.37), \tag{4}$$

where R is the incident solar radiation, and T is the mean monthly temperature (Celsius).

In a previous study the model has been applied in two catchments, Mahantango Creek in Pennsylvania and Winters' Run in Maryland, for characterizing subsurface contribution to runoff. In this study we will use the model-calculated hourly evaporation estimates for the above two catchments and aggregate them over the month, the time unit of our investigation of deriving evaporation using NDVI observations. Note that one cannot expect the vegetation to respond to changes in soil-moisture or atmospheric conditions overnight. A one-month time interval, however, may be large enough to let the vegetation adjust to changes in soil moisture and atmospheric conditions (Narasimha *et al.*, 1993).

In addition to the watershed model, a classical water balance model was applied for five catchments across the U.S. The model is a modified version (Vorosmarty *et al.*, 1989) of the classical Thornthwaite-Mather (1957) water-balance accounting procedure. Input data to the model include monthly sums of precipitation and radiation, monthly averages of temperature, dominant vegetation cover, and soil type of the catchment. At a monthly increment, the model makes predictions for potential evaporation, actual evaporation (E), soil-moisture content (SM), and runoff.

During months when precipitation (P) is in excess of PE, soil moisture can increase up to a maximum field capacity (FC) determined by soil texture and rooting depths. During dry months, when precipitation is exceeded by PE, soil moisture becomes a function of potential water loss. The relevant equations for soil-moisture calculations applied in the model are

$$\frac{d(SM)}{dt} = P - PE\ , \qquad if\ P > PE,\ SM < FC \tag{5}$$

$$\frac{d(SM)}{dt} = 0\ , \qquad if\ P > PE,\ SM = FC \tag{6}$$

$$\frac{d(SM)}{dt} = -\beta \cdot SM \cdot (PE - P)\ , \quad if\ P < PE, \tag{7}$$

where β is the slope of the moisture-retention function. The value of β can be calculated by

$$\beta = \frac{\ln(FC)}{(1.1282 \cdot FC)^{1.2756}} \tag{8}$$

which is an empirical formula for the slope of the moisture-retention function. This formula allows the retention function to behave differently for different soil types.

Once soil moisture is determined, evaporation is calculated. Following Thornthwaite and Mather (1957), E is set equal to PE in months, when precipitation is greater or equivalent to PE. During these months it is assumed that precipitation satisfies the water demands of the vegetation. During dry months, when precipitation is less than PE, the monthly sum of E is calculated as

$$E = P - \frac{d(SM)}{dt}, \qquad if\ P < PE, \tag{9}$$

During wet months, when field capacity is attained and the evaporation need of the vegetation is satisfied, the surplus water either seeps down into the soil to appear as groundwater recharge or runs off.

In addition to the above two watersheds (Mahantango Creek and Winters' Run), where both models were used, the catchments where the water-balance model was applied, are the Weeping Water, Nebraska, catchment and two watersheds in the Little River basin, Georgia, watersheds B and F (Figure 1). Watershed F is the headwater sub-basin of Watershed B in Georgia.

Figure 1. Locations of the Selected Watersheds.

Mahantango Creek in east-central Pennsylvania is a tributary of the Susquehanna River, which is located in the non-glaciated part of the North Appalachian Ridge and Valley Region. The watershed is characterized by long ridges of 300-400 m in elevation, alternating with broad valleys, 150-300 m in elevation. The geology of the Mahantango watershed can be described, from northwest to southeast, as folded Pennsylvanian sandstone and shale, Mississippian sandstone and shale, and Devonian sandstone, siltstone, and shale (NASA-EOS Report, 1995). The moderately weathered channery or stony loam soils, characteristic of the catchment, are thin with poorly developed horizons (ARS-USDA, 1976). The catchment area is 423 km^2. The catchment experiences a humid climate with an annual precipitation of 1,140 mm. The typical vegetation cover is mixed forest dominated by deciduous trees.

Winter's Run is a small, humid catchment (94 km^2) in northeastern Maryland draining into the Chesapeake Bay 20 km south of the Susquehanna River. It is located in the Piedmont region, which is characterized by gently rolling hills of metamorphic and igneous rock types (Schmidt, 1993). The silty loam soils covering the catchment are thin with poorly developed horizons (Schmidt, 1993). Annual precipitation is 1,020 mm; the predominant land use is crop and pasture.

Catchments B and F, near the town of Tifton, Georgia, in the Little River basin, are experimental watersheds operated by the U.S. Department of Agriculture. The watersheds are representative of the Coastal Plain Province of the eastern Unites States, which extends from New England along the Atlantic coast to Texas (Williams, 1985). Catchments B and F have a drainage area of 334 and 114 km^2, respectively. About half of the drainage area of each catchment is covered with mixed forests, while the other half is dryland crops and pasture (Sheridan, 1997). The watersheds are covered with Quaternary sediments, poorly-sorted sands interbedded with partly indurated sandy claystones and clays that are underlain by limestones over the Hawthorn Formation, an aquiclude at a depth of 1-3 m (ARS-USDA, 1976). The soils are permeable, and the infiltration rates are high (Williams, 1985). The surface topography is relatively flat (Shirmohamaddi *et al.*, 1986). Less than 2 percent of the annual precipitation of 1,200 mm is lost to deep percolation (Williams, 1985; Shirmohamaddi *et al.*, 1986). Climate in the region is characterized as humid subtropical with long, warm summers and short, mild winters (Sheridan, 1997). Precipitation occurs almost exclusively as rainfall throughout the year (Sheridan, 1997).

The Weeping Water catchment in eastern Nebraska has a drainage area of 624 km^2. It lies within the

Drift Hills region which is characterized by a rolling hill topography formed by glaciers in the Pleistocene. Loess in thick-to-thin deposits mantles the entire region, permitting moderate infiltration (CSD-UNL, 1998). The soils are deep, and moderately well drained. The climate of the area is typically continental with an average annual precipitation of about 800 mm, with the majority of the precipitation occurring in June. More than 80 percent of the watershed is cropland and pasture. Irrigation, unlike the rest of Nebraska, is negligible in the area, which is the most humid part of the state.

EVAPORATION ESTIMATION

For watersheds with varied vegetation types, catchment-scale evaporation rates under unlimited water supply conditions can be estimated by pan evaporation values modified by an appropriate coefficient (Brutsaert, 1982:214; Dunne and Leopold, 1978:127; Rodda *et al.*, 1976:113; Viessman *et al.*, 1989:101; Wilson, 1970:35-36). Published values of the pan coefficient for type A pans vary between .31 and 1.32 (Dunne and Leopold, 1978:101) and can be a function of the month. Evaporation under unlimited water supply becomes equal to potential evaporation (*PE*), which can be estimated by Equation (4). During wet months the pan coefficient-modified pan evaporation rate must equal *PE*. Figure 2 compares the two evaporation estimates during wet months in the Mahantango Creek, Pennsylvania, watershed. In dry months, neither the pan evaporation nor Equation (4) can estimate actual evaporation, since this latter one also becomes a function of soil moisture. A water balance/watershed model must be calibrated, usually against observed runoff, before meaningful E estimates can be obtained. Table 1 lists the explained variance (R^2) between monthly simulated and observed runoff values for each watershed using the calibrated water balance and the watershed model. The modeled runoff captures more than 80 percent of the variance in monthly runoff during the optimization period and about 70 percent in the verification period. The mean absolute error (MAE) is about 10 mm/month, which is about one- third of the mean standard deviation.

To check if spatially (over the watershed) averaged NDVI can be successfully converted into monthly evaporation estimates, the following has been done. The starting point coordinates of the NDVI versus evaporation relationship can be obtained by assigning an NDVI value to the assumed zero evaporation rate. Strictly speaking, watershed transpiration is very rarely zero, even during winter months, due to the widespread distribution of evergreen coniferous vegetation at practically any latitude. After applying a widely used transformation of adding one to each raw NDVI value of Equation (1) and multiplying it by 100 (Seevers and Ottmann, 1994; Di *et al.*, 1994), this value theoretically is 100, since the range of the original NDVI values is [0; 1] (Price, 1990). Seevers and Ottmann (1994), using Thematic Mapper data, found this value to be 105 in practice, while we found a value of 110 for the watersheds that have been selected for analysis (see Table 1 and Figure 1) using preprocessed (Yang *et al.*, 1997) monthly Maximum Value Composited 1-km resolution AVHRR data (USGS/EROS Data Center) for the period 1990-1997, except 1994, when NDVI values were not available for most of the year due to satellite problems. The two satellites use slightly different wavelengths to define NDVI (Seevers and Ottmann, 1994). The NDVI value of 110 also corresponds to the spatially averaged values of NDVI for the selected watersheds in January. This is because chlorophyll activity is reduced to close to zero during winter in the selected catchments.

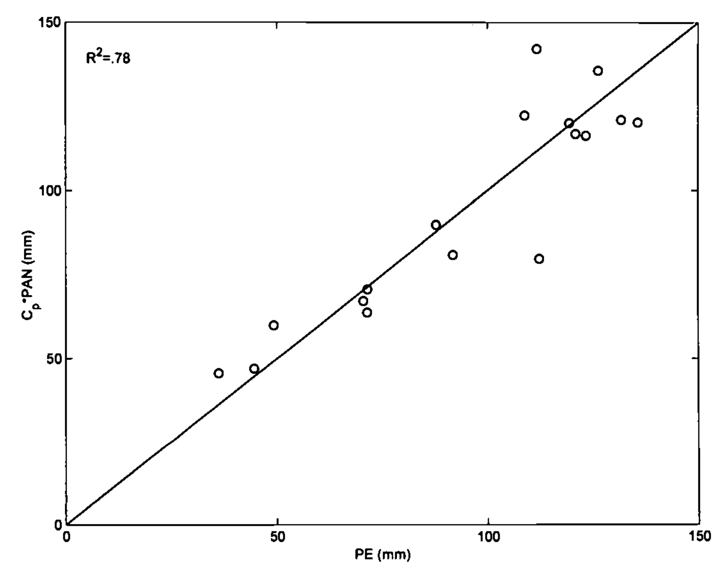

Figure 2. Monthly Potential Evaporation Versus Pan-Coefficient-Modified Evaporation Estimates, Manhantango Creek, Pennsylvania, May-October 1990-1992.

Next, the slope of the NDVI versus evaporation relationship had to be defined. This was accomplished by systematically changing the slope value in the equation and running the water balance model with the so-derived evaporation estimates. The slope value was retained that resulted in the highest correlation value between observed and modeled runoff and in the lowest mean absolute error. Table 1 lists the optimized linear transformations.

TABLE 1a. Model Performance Statistics, Optimization Period.

	Winter's Run Maryland	Mahantango Creek Pennsylvania	Watershed B Georgia	Watershed F Georgia	Weeping Water Nebraska
Area (km^2)	94	423	334	114	624
Optimization Period	1990-1993	1990-1993	1990-1993	1990-1993	1990-1993
$m_o (\sigma_o)$ [mm]	41.85 (23.76)	39.67 (39.72)	32.81 (46.23)	36.31 (48.56)	19.53 (48.11)
$m_{sM} (\sigma_{sM})$ [mm]	42.48 (20.19)	51.20 (32.41)	31.92 (44.93)	35.93 (48.72)	19.7 (47.07)
MAE_M [mm]	9.43	20.05	6.67	8.51	10.25
R_M^2; $< R_M^2 > = .83$	.70 .76*	.67 .83*	.94	.94	.90
$m_{sN} (\sigma_{sN})$ [mm]	41.91 (18.15)	40.01 (34.41)	33.03 (46.02)	36.12 (49.47)	19.60 (48.81)
MAE_N [mm]	8.77	13.20	7.70	10.38	11.05
R_N^2; $< R_N^2 > = .85$	.76	.77	.93	.90	.89
Estimated E vs NDVI Relationship	E = 1.7NDVI-187	E = 1.5NDVI-165	E = 3.6NDVI-396	E = 3.6NDVI-396	E = 3.07NDVI-338

TABLE 1b. Model Performance Statistics, Verification Period.

	Winter's Run Maryland	Mahantango Creek Pennsylvania	Watershed B Georgia	Watershed F Georgia	Weeping Water Nebraska
Verification Period	1995-1997	1995-1997	1995-1996	1995-1996	1995-1997
$m_o (\sigma_o)$ [mm]	53.15 (29.11)	48.54 (46.73)	19.26 (31.56)	21.61 (31.46)	10.20 (9.27)
$m_{sM} (\sigma_{sM})$ [mm]	55.11 (27.41)	50.17 (37.54)	16.12 (30.24)	17.57 (31.78)	6.61 (14.22)
MAE_M [mm]	12.64	18.93	6.85	7.44	9.59
R_M^2; $< R_M^2 > = .69$	.65 .70*	.67 .74*	.90	.87	.34
$m_{sN} (\sigma_{sN})$ [mm]	54.31 (24.19)	45.31 (34.39)	18.82 (35.58)	20.97 (34.62)	8.28 (16.06)
MAE_N [mm]	11.41	19.32	7.84	7.92	8.33
R_N^2; $< R_N^2 > = .73$	.62	.66	.86	.87	.65
R_X^2; $< R_X^2 >^* = .77$	.76 .81*	.78 .85*	.67	.63	.89

KEY: *m*: mean monthly runoff; σ: standard deviation of monthly runoff; *MAE*: mean absolute error between monthly observed and simulated runoff; *R*: correlation coefficient; *E*: monthly evaporation [mm]; < .>: average value, taken over the watersheds (excluding starred values); < .>*: average value, taken over the watersheds (including starred values).

KEY TO SUBSCRIPTS: *o*: observed value; *s*: model-simulated value; *M*: water balance-modeled runoff; *N*: water balance-modeled runoff using linearly transformed NDVI for monthly evaporation estimation instead of model simulated one; *X*: water balance model-simulated and NDVI-derived monthly evaporation estimates.

KEY TO SUPERSCRIPTS: *: values obtained by using the watershed model outputs.

RESULTS AND DISCUSSION

The results of comparing model-calculated and NDVI-derived monthly evaporation estimates can be found in Table 1. The mean R^2 value taken over the five watersheds between the two variables is .77, which translates to a mean correlation coefficient of almost .9. In the least humid watershed, the Weeping Water catchment in Nebraska, the highest correlation resulted when the evaporation values calculated by the water-balance model were shifted one month later, compared to the NDVI-derived estimates, similar to what has been reported by Szilagyi *et al.* (1998) in the case of a semi-arid watershed in western Nebraska. Kerr *et al.* (1989) and Cihlar *et al.* (1991) found similar shifts in their NDVI and model-evaporation data. The existence of this shift pinpoints the important role vegetation plays in soil-moisture regulation with increasing aridity of the prevailing climate. Figure 3 displays the one-month-shifted model- and NDVI-derived monthly evaporation estimates. In Figure 4 the two variables are plotted against each other with the 1:1 line shown. Very similar graphs to Figures 3 and 4 can be obtained for the remaining watersheds with concurrent monthly data. Table 1 summarizes the results.

Figures 3 and 4 do not tell which evaporation estimate is closer to reality. In the lack of measurable watershed evaporation, NDVI-derived evaporation estimates have routinely been compared to model-calculated values (Kerr *et al.*, 1989; Cihlar *et al.*, 1991). Since these latter ones are prone to potentially large errors, such as the NDVI-derived evaporation values, comparing two variables with unknown errors does not seem to be the best way to proceed. To decide which one is a better representation of reality one could use the two estimates and check how a model, using the estimates, captures runoff, which can generally be measured. Table 1 shows (see the R^2 and MAE values) that the NDVI-derived evaporation estimates result in at least the same accuracy of runoff simulation as the model-generated evaporation estimates.

Insofar one had to rely on some kind of a hydrologic model to transform the watershed-averaged NDVI values into monthly watershed evaporation estimates through optimizing model simulated runoff. Since the resulting evaporation values are of about the same accuracy as the model-calculated evaporation estimates, there seems to be not much to be gained by using NDVI. The real advantage, however, of using NDVI comes around when lack of data prohibits any hydrologic model applications. Such may be the case when runoff data are missing or when irrigation is significant in the area of interest, but its level is unknown. This is typical of Nebraska, which is among the leading states in the U.S. in irrigated acreage and water volumes and where the law does not require farmers to document their agricultural water consumption. In such a situation, NDVI may still provide an alternative for estimating watershed evaporation, as described below.

It was mentioned earlier that watershed evaporation can be estimated by pan evaporation rates in non-water-stressed periods through the application of a pan coefficient. Figures 5a-e display the pan

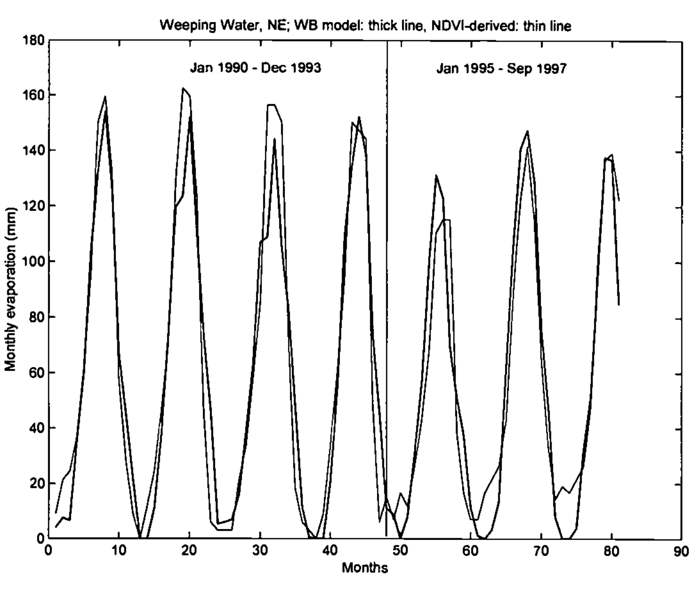

Figure 3. Model Simulated and NDVI-Derived Monthly Evaporation Estimates, Weeping Water, Nebraska.

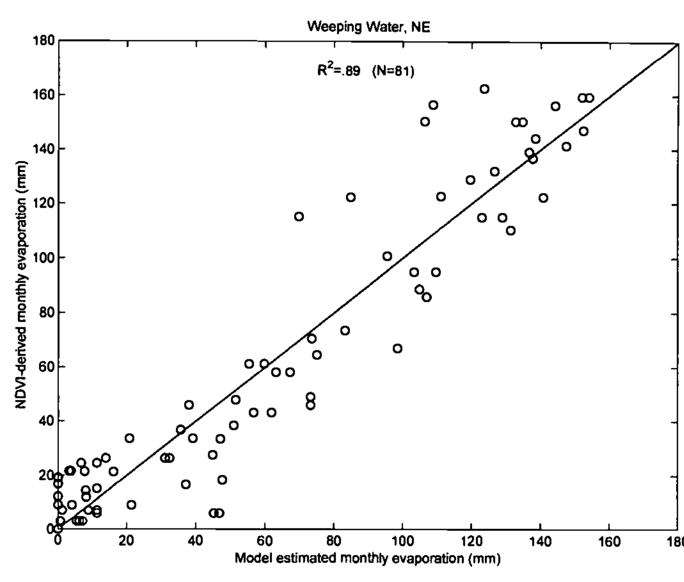

Figure 4. Model Simulated Versus NDVI-Derived Monthly Evaporation Estimates, Weeping Water, Nebraska.

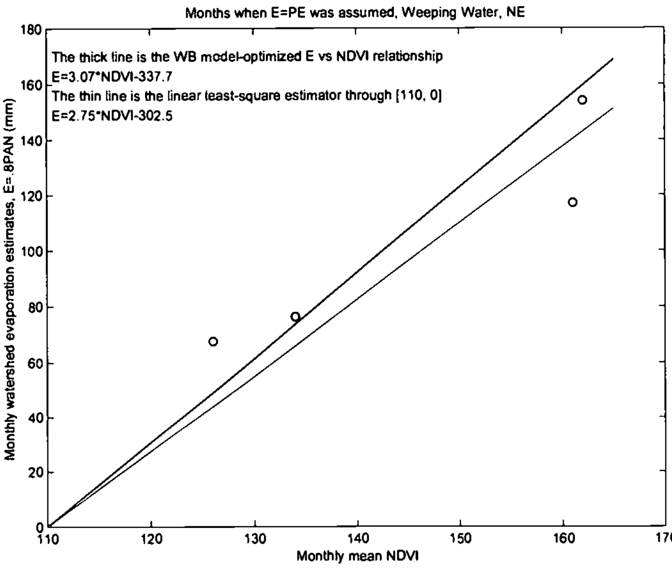

(a)

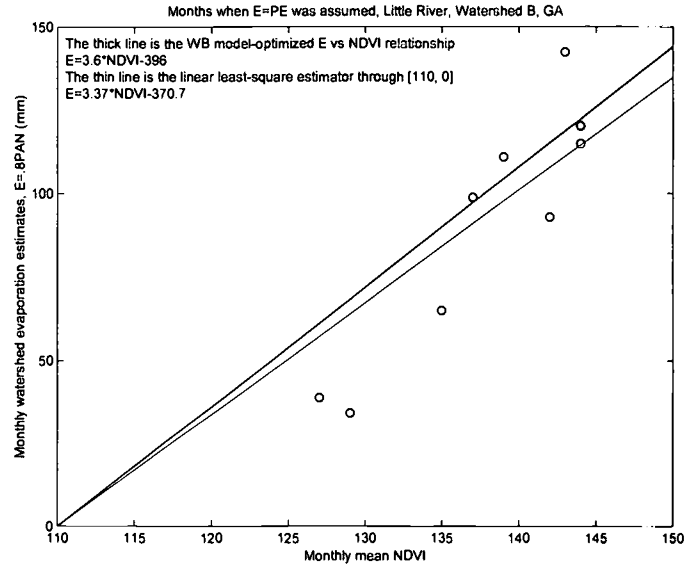

(b)

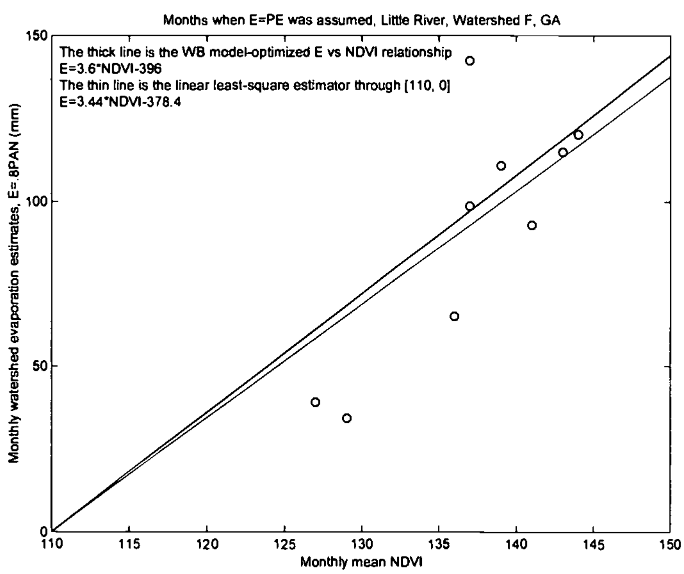

(c)

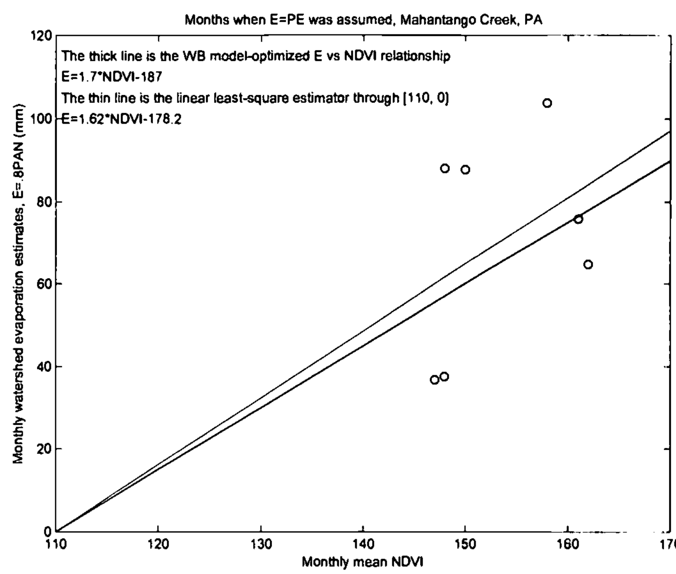

(d)

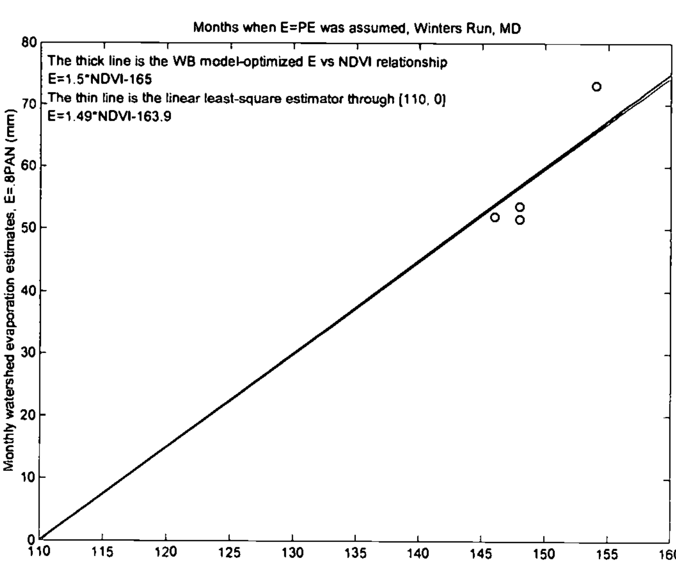

(e)

Figure 5. Pan Coefficient-Modified Pan Evaporation Versus Watershed-Averaged NDVI in Wet Months. The thick line is the water-balance model-optimized NDVI-vs-evaporation relationship; the thin line is the linear least-square estimator going through [110, 0]. (a) Weeping Water, Nebraska; (b) Watershed B, Little River, Georgia; (c) Watershed F, Little River, Georgia; (d) Mahantango Creek, Pennsylvania; (f) Winters' Run, Maryland.

evaporation values, reduced by the most frequently chosen pan coefficient value of .8 (Dunne and Leopold, 1978:134) and plotted against NDVI values for months with abundant soil moisture (i.e., when precipitation was unexpectedly high in the previous month). The same graphs contain the water balance-optimized NDVI-evaporation lines (thick). As can be seen, the water balance model-optimized NDVI-evaporation equations are very close to the ones one can obtain by drawing a (thin) line from the origin [110, 0] of the graphs that minimizes the scatter between this line and the observed data points. It means that without resorting to any hydrologic model the sought-after NDVI-evaporation relationship can be determined by simply using NDVI and pan evaporation observations during wet months. As a consequence, watershed evaporation can be estimated using only precipitation, pan evaporation and NDVI records, even in cases when missing hydrological data prohibits hydrologic model applications.

In summary, NDVI-derived monthly watershed evaporation estimates were validated via the application of a water-balance model using the NDVI-derived evaporation values in the model and comparing the simulated runoff with observational data. The linear transformation of watershed-averaged monthly Maximum Value Composited NDVI values into monthly evaporation estimates proved to be at least as accurate as the classical evaporation estimation method of the Thornthwaite-Mather (1957) water balance accounting procedure in combination with the Jensen-Haise (1963) technique. A promising advantage of applying NDVI data for monthly areal evaporation assessment over hydrologic/water balance models is that the former does not have the typical data input requirement of a hydrologic/water balance model, which, in turn, means a possibly broader range of practical applicability.

ACKNOWLEDGMENTS

The authors are thankful to Franz Mora for providing them with the NDVI data and to Charles Flowerday for his editing. Partial support from an EPA grant on climate change and human health is also gratefully acknowledged. The authors are grateful to Joseph M. Sheridan of the USDA Southeast Watershed Research Laboratory for his and his team's help with data acquisition.

LITERATURE CITED

ARS-USDA, 1976. Miscellaneous Publications. Nos. 1330, 1464, 1469, Washington, D.C.

Beven, K. J., 1991. Scale Considerations. *In:* Recent Advances in the Modeling of Hydrologic Systems, D. S. Bowles and P. E. O'Connell (Editors). Kluwer Academic, Dordrecht, p. 667.

Brutsaert, W., 1982. Evaporation Into the Atmosphere: Theory, History and Applications. D. Reidel, Norwell, Massachusetts, p. 229.

Bunce, J. A., 1997. Does Transpiration Control Stomatal Responses to Water Vapour Pressure Deficit? Plant Cell Environ., 20:131-135.

Chauhan, N. S., 1997. Soil Moisture Estimation Under a Vegetation Cover: Combined Active, Passive Microwave Remote Sensing Approach. Int'l. J. Remote Sens. 18:1079-1097.

Chen, D. Y., E. T. Engman, and W. Brutsaert, 1997. Spatial Distribution and Pattern Persistence of Surface Soil Moisture and Temperature Over Prairie from Remote Sensing. Remote Sens. Environ. 61:347-360.

Choudhury, B. J. and R. E. Golus, 1988. Estimating Soil Wetness Using Satellite Data. Int'l. J. Remote Sens. 8:1085-1090.

Choudhury, B. J. and C. J. Tucker, 1987. Monitoring Global Vegetation Using Nimbus-7 37 GHz Data: Some Empirical Relations. Int'l. J. Remote Sens. 8:1085-1090.

Cihlar, J., L. St-Laurent, and J. A. Dyer, 1991. Relation Between the Normalized Difference Vegetation Index and Ecological Variables. Remote Sens. Environ. 35:279-298.

Committee on Opportunities in the Hydrologic Sciences, Water Science and Technology Board, Commission on Geosciences, Environment, and Resources, and National Research Council, 1991. Opportunities in the Hydrologic Sciences. National Academy Press, Washington D.C., p. 155.

Conservation and Survey Division, 1998. The Groundwater Atlas of Nebraska. University of Nebraska-Lincoln, Lincoln, Nebraska, p. 44.

Crago, R. D. and W. Brutsaert, 1992. A Comparison of Several Evaporation Equations. Water Resour. Res. 28:951-954.

Davenport, M. L. and S. E. Nicholson, 1993. On The Relationship Between Rainfall and Normalized Difference Vegetation Index for Diverse Vegetation Types in East Africa. Int'l. J. Remote Sens. 14:2369-2389.

Desborough, C. E., 1997. The Impact of Root Weighting on the Response of Transpiration to Moisture Stress in Land Surface Schemes. Month. Weather Rev. 125:1,920-1,930.

Desjardins, R. L., P. H. Schuepp, J. I. MacPherson, and D. J. Buckley, 1992. Spatial and Temporal Variations of the Fluxes of Carbon Dioxide and Sensible and Latent Heat Over the FIFE Site. J. Geophys. Res. 97(18):467-18,475.

Di, L., D. C. Rundquist, and L. Han, 1994. Modeling Relationships Between NDVI and Precipitation During Vegetative Growth Cycles. Int'l. J. Remote Sens. 15:2,121-2,136.

Dunne, T. and L. B. Leopold, 1978. Water in Environmental Planning. W. H. Freeman and Company, San Francisco, California, p. 818.

Eichinger, W., D. Cooper, D. Holtkamp, R. Karl, Jr., J. Moses, C. Quick, and J. Tiee, 1993a. Derivation of Water Vapor Fluxes from Lidar Measurements. Boundary Layer Meteor. 63:39-64.

Eichinger, W., D. Cooper, M. B. Parlange, and G. G. Katul, 1993b. The Application of a Scanning, Water-Raman Lidar as a Probe of the Atmospheric Boundary Layer. IEEE Trans. Geosci. Remote Sens. 31(1):70-79.

Eichinger, W., D. Cooper, F. Archuleta, D. Hof, D. Holtkamp, R. Karl, Jr., C. Quick, and J. Tiee, 1994. Development and Application of a Scanning, Solar-Blind Water Raman-Lidar. Applied Optics 33:3923-3932.

Farrar, T. J., S. E. Nicholson, and A. R. Lare, 1994. The Influence of Soil Type on the Relationships Between NDVI, Rainfall, and Soil Moisture in Semi-Arid Botswana. II. Relationship to Soil Moisture. Remote Sens. Environ. 50:121-131.

Galchen, T., M. Xu, and W. L. Eberhard, 1992. Estimations of Atmospheric Boundary Layer Fluxes and Other Turbulence Parameters from Doppler Lidar Data. J. Geophys. Res. 97: 18,409-18,423.

Gao, W., M. L. Wesely, D. R. Cook, and R. L. Hart, 1992. Air-Surface Exchange of H_20, CO_2, and O_3 at a Tallgrass Prairie in Relation to Remotely Sensed Vegetation Indices. J. Geophys. Res. 97:18,663-18,671.

Granier, A., P. Biron, N. Breda, and J. Y. Pontailler, 1996. Transpiration of Trees and Forest Stands – Short and Long-Term Monitoring Using Sapflow Methods. Global Change Biology 2:265-274.

Grist, J., S. E. Nicholson, and A. Mpolokang, 1997. On the Use of NDVI for Estimating Rainfall Fields in the Kalahari of Botswana. J. Arid Environ. 35:195-214.

Henricksen, B. L. and J. W. Durkin, 1986. Growing Period and Drought Early Warning in Africa Using Satellite Data. Int'l. J. Remote Sens. 7:1,583-1,608.

Jackson, T. J., J. Schmugge, and E. T. Engman, 1996. Remote Sensing Applications to Hydrology-Soil Moisture. Hydrol. Sci. J. 41: 517-530.

Jensen, M. and H. Haise, 1963. Estimating Evapotranspiration from Solar Radiation. ASCE J. Irrig. Drainage 89:5-41.

Kaimal, J. C. and J. J. Finnigan, 1994. Atmospheric Boundary Layer Flows: Their Structure and Measurement. Oxford University Press, New York, New York, p. 289.

Kerr, Y. H., J. Imbernon, G. Dedieu, O. Hautecoeur, J. P. Lagouarde, and B. Seguin, 1989. NOAA AVHRR and Its Uses for Rainfall and Evapotranspiration Monitoring. Int'l. J. Remote Sens. 10:847-854.

Koster, R. D. and P. C. D. Milly, 1997. The Interplay Between Transpiration and Runoff Formulations in Land Surface Schemes Used with Atmospheric Models. J. Climate 10:1,578-1,591.

Lafleur, P. M., A. B. Wurtele, and C. R. Duguay, 1997. Spatial and Temporal Variations in Surface Albedo of a Subarctic Landscape Using Surface-Based Measurements and Remote Sensing. Arctic and Alpine Res. 29:261-269.

Luthi, D., C. Schar, C. Frei, and H. C. Davies, 1997. The Influence of Initial Soil Moisture Upon the Hydrological Cycle in a Regional Climate Model. 13th Conference on Hydrology, Long Beach, Calfiornia

Maidment, D. R. (Editor), 1993. Handbook of Hydrology. McGraw-Hill, New York, New York, Chapter 29.

Narasimha, P. V., L. Venkataratnam, P. V. Krishna, and K. V. Ramanam 1993. Relation Between Root Zone Soil Moisture and Normalized Difference Vegetation Index of Vegetated Fields. Int'l. J. Remote Sens. 14:441-449.

NASA-EOS Progress Report, 1995. Global Water Cycle: Extention Across the Earth Sciences. NAGW-2686.

Nicholson, S. E., M. L. Davenport, and A. R. Malo, 1990. A Comparison of the Vegetation Response to Rainfall in the Sahel and East Africa, Using Normalized Difference Vegetation Index from NOAA AVHRR. Climate Change 17:209-241.

Nicholson, S. E. and T. J. Farrar, 1994. The Influence of Soil Type on the Relationships Between NDVI, Rainfall, and Soil Moisture in Semi-Arid Botswana. I. Relationsh to Rainfall. Remote Sens. Environ. 50:107-120.

Nicholson, S. E., A. R. Lare, J. A. Marengo, and P. Santos, 1996. A Revised Version of Lettau's Evapoclimatonomy Model. J. Applied Meteor. 35:549-561.

Parlange, M. B., W. E. Eichinger, and J. D. Albertson, 1995. Regional Scale Evaporation and the Atmospheric Boundary Layer. Rev. Geophys. 33(1):99-124.

Parlange, M. B. and G. G. Katul, 1995. Watershed Scale Shear Stress from Tethersonde Wind Profile Measurements Under Near Neutral and Unstable Atmospheric Stability. Water Resour. Res. 31:961-968.

Prazak, J., M. Sir, and M. Tesar, 1996. Parameters Determining Plant Transpiration Under Conditions of Sufficient Soil Moisture. J. Hydrol. 183:425-431.

Price, J. C., 1990. Using Spatial Context in Satellite Data to Infer Regional Scale Evapotranspiration. IEEE Trans. Geosci. Remote Sens. 28:940-948.

Quintarelli, F., 1993. Acoustic Sounder Observations of Atmospheric Turbulence Parameters in a Convective Boundary Layer. J. Applied Meteor. 32:1433-1440.

Ralph, F., C. Mazaudier, M. Crochet, and S. Venkateswaran, 1993. Doppler Sodar and Radar Wind-Profiler Observations of Gravity-Wave Activity Associated with a Gravity Current. Mont. Weather Rev. 121:44-463.

Rodda, J. C., R. A. Downing, and F. M. Law, F. M., 1976. Systematic Hydrology. Newnes-Butterworths, London, p. 399.

Running, S. W. and R. R. Nemani, 1988. Relating Seasonal Patterns of the AVHRR Vegetation Index to Simulated Photosynthesis and Transpiration of Forests in Different Climates. Remote Sens. Environ. 24:347-367.

Schmidt, Jr., M. F., 1993. Maryland's Geology. Tidewater Publishers, Centreville, Maryland, p. 145.

Schreiber, L. and M. Riederer, 1996. Ecophysiology of Cuticular Transpiration – Comparative Investigation of Cuticular Water Permeability of Plant Species from Different Habitats. Oecologia 107:426-432.

Schultz, P. A. and M. S. Halpert, M. S., 1993. Global Correlation of Temperature, NDVI, and Precipitation. Advanc. Space Res. 13:277-280.

Seevers, P. M. and R. W. Ottmann, 1994. Evapotranspiration Estimation Using a Normalized Difference Vegetation Index Transformation of Satellite Data. Hydrol. Sci. J. 39:333-345.

Seguin, B., E. Assad, J. P. Freteaud, J. Imbernon, Y. Kerr, and J. P. Lagouarde, 1989. Use of Meteorological Satellites for Water Balance Monitoring in Sahelian Regions. Int'l. J. Remote Sens. 10: 1,101-1,117.

Sellers, P. J., 1985. Canopy Reflectance, Photosynthesis, and Transpiration. Int'l. J. Remote Sens. 6:1,335-1,372.

Shirmohamaddi, A., J. M. Sheridan, and L. E. Asmussen, 1986. Hydrology of Alluvial Stream Channels in Southern Coastal Plain Watersheds. Trans. ASAE 29:135-142.

Sheridan, J. M., 1997. Rainfall-Streamflow Relations for Coastal-Plain Watersheds. Appl. Eng. Agric. 13:333-344.

Smith, J. A., N. S. Chauhan, T. J. Schmugge, and J. R. Ballard, 1997. Remote Sensing of Land Surface Temperature: The Directional Viewing Effect. IEEE Trans. Geosci. Remote Sens. 35:972-974.

Szilagyi, J. and M. B. Parlange, 1999. A Geomorphology-Based Semi-Distributed Watershed Model. Advanc. Water Resour. (in print).

Szilagyi, J., M. B. Parlange, D. C. Rundquist, and D. C. Gosselin, 1998. NDVI Relationship to Monthly Evaporation. Geophys. Res. Letters 25(10):1753-1756.

Tarpley, J. D., S. R. Schneider, and R. L. Money, 1984. Global Vegetation Indices from the NOAA-7 Meteorological Satellite. J. Climate and Appl. Meteor. 23:491-494.

Thomas, P. and S. Vogt, 1993a. Intercomparison of Turbulence Data Measured by Sodar and Sonic Anemometers. Boundary Layer Meteor. 62:353-359.

Thomas, P. and S. Vogt, S., 1993b. Variances of the Vertical and Horizontal Wind Measured by Tower Instruments and Sodar – An Intercomparison. Appl. Phys., B, 57:19-26.

Thornthwaite, C. W. and J. R. Mather, 1957. Introduction and Tables for Computing Potential Evapotranspiration and the Water Balance. Drexel Institute of Technology, Publ. Climat., X, 3:205-209.

Tucker, C. J., J. H. Elgies, J. E. McMurtrey, and C. J. Fan, 1979. Monitoring Corn and Soybean Crop Development with Hand-Held Radiometric Spectral Data. Remote Sens. Environ. 8:237-248.

Tucker, C. J., C. L. Vanpraet, M. J. Sharman, and G. Ittersum, 1985. Satellite Remote Sensing of Total Herbaceous Biomass Production in the Senegalese Sahel: 1980-1984. Remote Sens. Environ. 17:233-249.

Viessman, W. Jr., G. L. Lewis, and J. W. Knapp, 1989. Introduction to Hydrology. Harper and Row, New York, New York, p. 780.

Vorosmarty, C., B. Moore, A. L. Grace, and P. Gildea, P., 1989. Continental-Scale Models of Water Balance and Fluvial Transport: An Application to South America. Global Biogeochem. Cycles 3:34-43.

Walsh, S. J., 1987. Comparison of NOAA AVHRR Data to Meteorologic Drought Indices. Photogram. Eng. Remote Sens. 53:1,069-1,074.

Wiegand, C. L. and A. J. Richardson, A. J., 1990. Use of Spectral Vegetation Indices to Infer Leaf Area, Evapotranspiration, and Yield. Agronomy J. 82:623-629.

Williams, R. G., 1985. Watershed Evapotranspiration Prediction Using the Blaney-Criddle Approach. Trans. ASAE 28:1,856-1,860.

Wilson, E. M., 1970. Engineering Hydrology. John Wiley and Sons, New York, New York, p. 232.

Wittich, K. P. and O. Hansing, 1995. Area-Averaged Vegetative Cover Fraction Estimated from Satellite Data. Int'l. J. Biometrica 38:209-215.

Yang, W., L. Yang, and J. W. Merchant, 1997. An Assessment of AVHRR/NDVI-Ecoclimatological Relations in Nebraska, U.S.A. Int'l. J. Remote Sens. 18:2,161-2,180.